© 2017. Published by The Company of Biologists Ltd | Development (2017) 144, 1600-1606 doi:10.1242/dev.135681

FGFR2 is required for airway basal cell self-renewal and terminal differentiation

Gayan I. Balasooriya[1,*], Maja Goschorska[1], Eugenia Piddini[1,2] and Emma L. Rawlins[1,3,‡]

ABSTRACT

Airway stem cells slowly self-renew and produce differentiated progeny to maintain homeostasis throughout the lifespan of an individual. Mutations in the molecular regulators of these processes may drive cancer or degenerative disease, but are also potential therapeutic targets. Conditionally deleting one copy of FGF receptor 2 (FGFR2) in adult mouse airway basal cells results in self-renewal and differentiation phenotypes. We show that FGFR2 signalling correlates with maintenance of expression of a key transcription factor for basal cell self-renewal and differentiation: SOX2. This heterozygous phenotype illustrates that subtle changes in receptor tyrosine kinase signalling can have significant effects, perhaps providing an explanation for the numerous changes seen in cancer.

KEY WORDS: Cre-Lox, Lung, Mouse, Trachea, Progenitor

INTRODUCTION

Like human airways, the mouse trachea contains three major epithelial lineages (Rock et al., 2010; Teixeira et al., 2013). Basal cells (BCs) are a stem cell population and include slowly dividing stem cells and committed luminal precursors (Mori et al., 2015; Rock et al., 2009; Watson et al., 2015). Luminal secretory cells self-renew and produce terminally differentiated ciliated cells (Rawlins and Hogan, 2008; Rawlins et al., 2007, 2009). Multiple studies have shown that SOX2 is a key transcription factor (TF) for the development and maintenance of all airway epithelial cells (Gontan et al., 2008; Hashimoto et al., 2012; Ochieng et al., 2014; Que et al., 2009; Tompkins et al., 2009, 2011). Deletion of *Sox2* in adult mouse tracheal epithelium caused loss of differentiated cells. Moreover, the $Sox2^{\Delta/\Delta}$ BCs were less able to proliferate *in vitro* or *in vivo* following injury (Que et al., 2009). SOX2 is thus required for BC self-renewal and luminal differentiation. SOX2 overexpression can be a driver of squamous cell carcinoma, which has a predominantly basal cell phenotype (Correia et al., 2017; Ferone et al., 2016).

FGFR2 function has been extensively studied during lung branching where one of its roles is to maintain undifferentiated epithelial progenitors by inhibiting SOX2 expression (Abler et al., 2009; Que et al., 2007; Volckaert et al., 2013). However, at later stages of embryonic development ectopic FGF10 can promote BC differentiation in $SOX2^+$ airway progenitors (Volckaert et al., 2013). The same study expressed a secreted dominant-negative FGFR2 in the late stages of embryogenesis and suggested that there could be a role for FGFR2 signalling in maintenance of airway BCs. We have now specifically tested this hypothesis in the steady-state adult mouse trachea, and show that FGFR2 is required for BC self-renewal and terminal differentiation. Moreover, FGFR2 signalling maintains SOX2 expression.

RESULTS AND DISCUSSION

FGFR2 is required for normal tracheal homeostasis

We detected FGFR2 protein in airway basal cells and at the apical surface of secretory cells (Fig. 1A,B), confirming previous results (Watson et al., 2015). To determine the role of FGFR2 in BCs, we conditionally deleted one copy of *Fgfr2* and activated a GFP reporter in adult tracheal BCs using *Tg(KRT5-CreER); Rosa26R*$^{fGFP/+}$*; Fgfr2*$^{fx/+}$ (*Fgfr2* conditional heterozygous, cHet) and control *Tg(KRT5-CreER); Rosa26R*$^{fGFP/+}$ mice (Fig. 1C). To test for co-recombination between *Fgfr2*^{fx} and the reporter, we isolated GFP^+ BCs by flow cytometry as GFP^+, GSIβ4-lectin$^+$ cells at 3 weeks post-tamoxifen (tmx) induction and performed RT-qPCR for *Fgfr2* (Fig. 1D). This confirmed that cHet BCs had ∼50% of the control *Fgfr2* mRNA level. Hence, we use GFP^+ cells as a surrogate marker for $Fgfr2^{\Delta/+}$ cells, being aware that co-recombination will not be 100%. Tracheae were harvested at intervals to assess the contribution of GFP^+, $Fgfr2^{\Delta/+}$ BCs to the epithelium during homeostatic turnover (Fig. 1E). At 1.5 weeks post-tmx, ∼30% of total BCs were GFP^+ in *Fgfr2*cHet and control mice. In controls, this percentage increased to ∼60% at 5 weeks post-tmx, before dropping to initial levels by 24 weeks. By contrast, in the *Fgfr2*cHet tracheae, the percentage of GFP^+ BCs remained approximately constant at 5 weeks, but decreased to less than 5% of total basal cells by 24 weeks (Fig. 1F). In both genotypes, labelled BCs produced labelled luminal cells. Luminal differentiation initially appeared more rapid in the *Fgfr2*cHets. However, luminal cell production was not sustained over time, likely due to the loss of GFP^+ BCs, and by 24 weeks the percentage of labelled luminal cells was significantly lower in the *Fgfr2*cHet tracheae (Fig. 1G).

This showed that *Fgfr2*cHet BCs can produce luminal cells, but that mutant basal and luminal cells are gradually lost. One possible reason for the loss of *Fgfr2*cHet cells is differential fitness and competition with neighbouring wild-type cells (Vivarelli et al., 2012). To test this, we mixed pure populations of *Rosa26R*$^{tdTomato/+}$*; Fgfr2*$^{\Delta/+}$ with unlabelled $Fgfr2^{+/+}$ BCs (1:2 ratio) and assessed their ability to compete *in vitro* at steady-state and following injury. We were unable to find evidence for differential proliferation or survival in the mixed cultures and conclude that it is unlikely that cell competition contributes to the observed loss of mutant cells (Fig. S1; Movies 1-5).

[1]Wellcome Trust/CRUK Gurdon Institute, University of Cambridge, Cambridge, CB2 1QN, UK. [2]School of Cellular and Molecular Medicine, Faculty of Biomedical Sciences, University of Bristol, Biomedical Sciences Building, University Walk, Bristol, BS8 1TD, UK. [3]Wellcome Trust/MRC Stem Cell Institute and Department of Pathology, University of Cambridge, Cambridge, CB2 1QN, UK.
*Present address: Cold Spring Harbor Laboratory, 1 Bungtown Road, Cold Spring Harbor, NY 11724, USA.

‡Author for correspondence (e.rawlins@gurdon.cam.ac.uk)

G.I.B., 0000-0002-0916-6686; E.L.R., 0000-0001-7426-3792

Received 24 January 2016; Accepted 15 March 2017

Development (2017) 144, 1600-1606 doi:10.1242/dev.135681

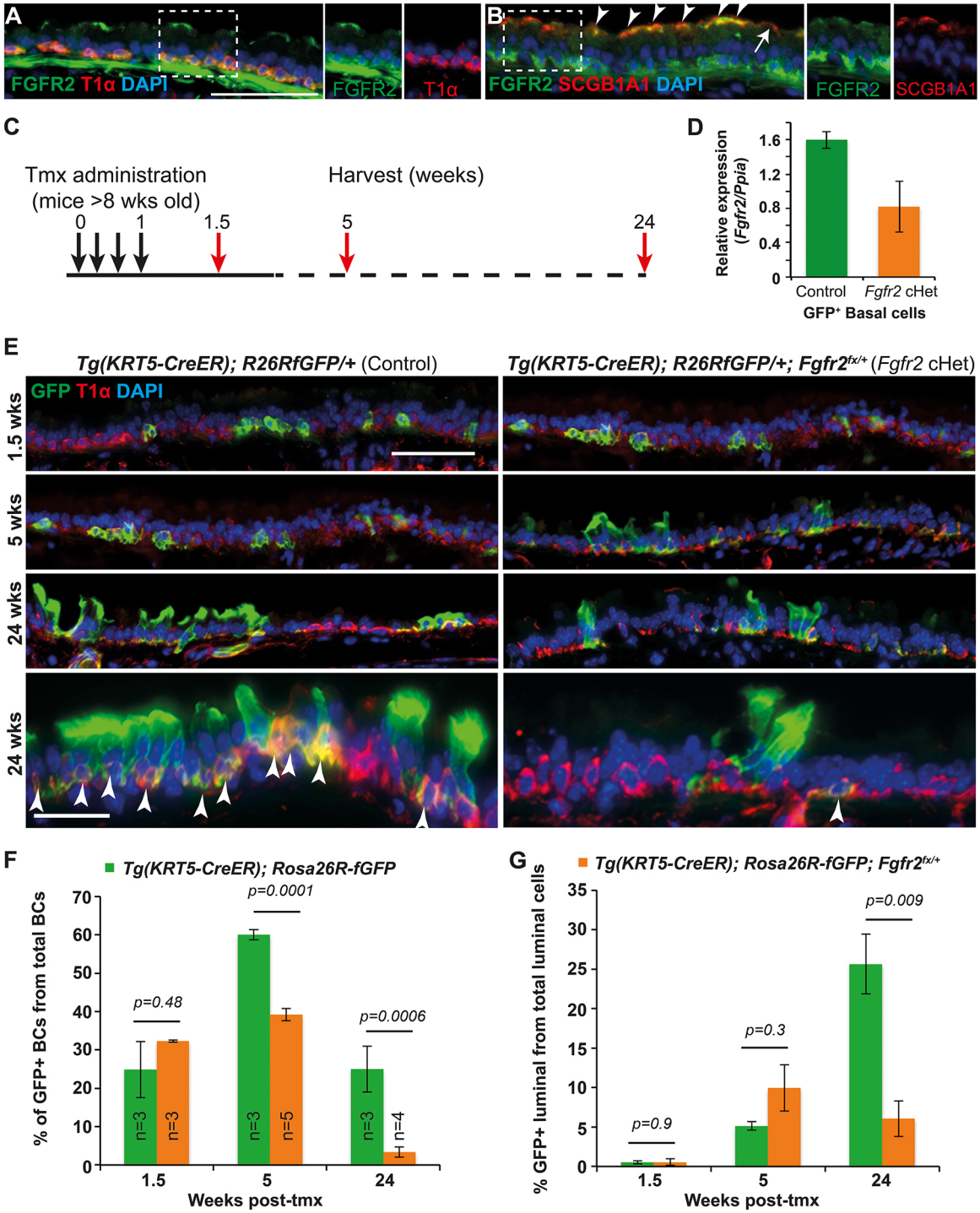

Fig. 1. Decreasing *Fgfr2* levels in basal cells results in altered tracheal homeostasis. (A,B) Adult tracheal sections. (A) Green, FGFR2; red, T1α (basal cells). (B) Green, FGFR2; red, SCGB1A1 (secretory cells). FGFR2$^+$ secretory cells (arrowheads); rare SCGB1A1$^+$, FGFR2$^-$ cells (arrow). (C) Experimental schematic. (D) Relative expression of *Fgfr2* mRNA in GFP$^+$ basal cells from control and *Fgfr2*cHet mice 3 weeks post-tmx. (E) Representative sections from control *Tg(KRT5-CreER); Rosa26R$^{fGFP/+}$* and cHet *Tg(KRT5-CreER); Rosa26R$^{fGFP/+}$; Fgfr2$^{fx/+}$* tracheae. Green, GFP (*Rosa* reporter); red, T1α (basal cells). Arrowheads indicate GFP$^+$ basal cells. (F,G) Percentage of the total T1α$^+$ BCs that are also GFP$^+$ (F) and percentage of the total T1α$^-$ luminal cells that are also GFP$^+$ (G). Blue, DAPI. Error bars indicate s.e.m. Scale bars: 50 µm.

*Fgfr2*cHet BCs do not differentiate into fully mature luminal cells

We asked whether the loss of *Fgfr2*cHet cells was due to a decrease in cell division. As expected, proliferation rates were low in all tracheae, but dividing GFP$^+$ cells were observed (Fig. S2A). We noted an increase in proliferation of the *Fgfr2*cHet GFP$^+$ cells at 1.5 weeks post-tmx, although this was not statistically significant and the change was not sustained over time (Fig. S2B). Thus, altered proliferation does not explain the phenotype. We also assessed apoptosis using cleaved caspase 3 staining, but did not identify caspase 3$^+$ cells (665 GFP$^+$ cells scored in four independent 5 week samples; Fig. S2C,D).

Development (2017) 144, 1600-1606 doi:10.1242/dev.135681

We assessed the ability of *Fgfr2*cHet cells to differentiate by analysing the luminal (KRT8) and basal (KRT5) cytokeratins at 5 weeks post-tmx (Fig. 2A). A higher percentage of the total GFP$^+$ cells co-stained with KRT8 in the mutants, indicating that more cells had begun differentiation to a luminal fate (Fig. 2B). Similarly, plotting the GFP/T1α staining (Fig. 1D) as a percentage of GFP$^+$ cells (GFP$^+$, T1α$^-$) showed more differentiating cells in the mutants (Fig. 2B). Thus, *Fgfr2*cHet cells exit the basal layer at a greater rate than controls and their descendants take on a luminal KRT8$^+$, T1α$^-$ fate, suggesting a self-renewal defect.

At steady-state, BCs initially differentiate into secretory cells that later produce ciliated cells (Watson et al., 2015). Cell fate analysis at 5 weeks post-tmx showed that both control and *Fgfr2*cHet BCs produce secretory SCGB1A1$^+$ cells (Fig. 2C,D). Moreover, there were no signs of goblet cell production in the mutants (Fig. 2C; n=4 MUC5AC^{lo} cells observed from 859 cells counted in 5 *Fgfr2*cHet individuals). However, analysis of acetylated tubulin-positive cilia (marker of terminal luminal differentiation) at 24 weeks post-tmx showed that the *Fgfr2*cHet cells never took on a ciliated cell identity (Fig. 2E).

*Fgfr2*cHet BCs have high levels of β-galactosidase activity *in vitro*

We tested the ability of *Fgfr2*cHet cells to proliferate and differentiate *in vitro* using a high dose of an adenovirus containing CMV-Cre (Ad-Cre) to recombine *Rosa26R*$^{fGFP/+}$; *Fgfr2*$^{fx/+}$ and control *Rosa26R*$^{fGFP/fGFP}$ BCs grown in self-renewing conditions

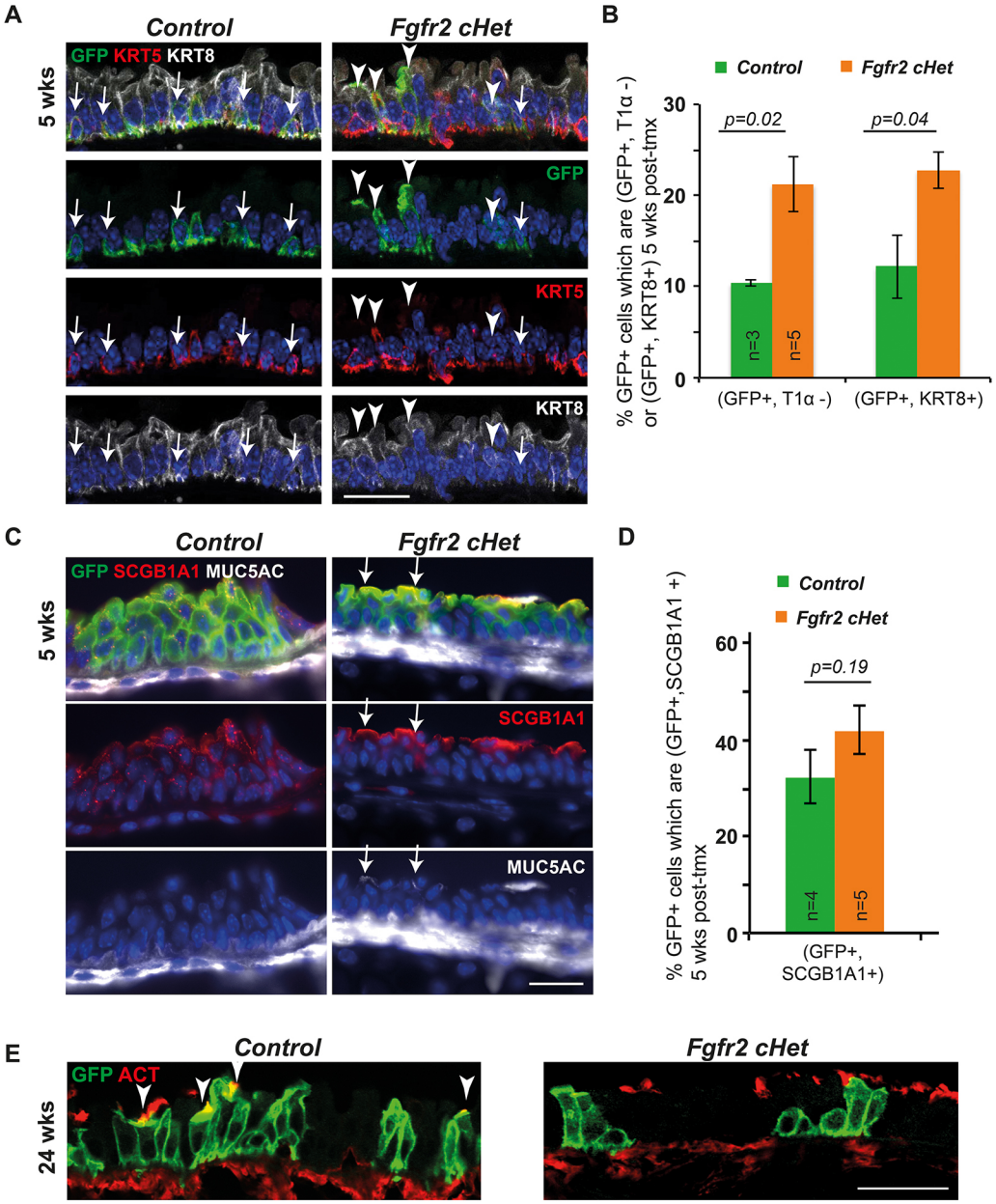

Fig. 2. *Fgfr2* conditional heterozygous basal cells do not produce terminally differentiated luminal cells. (A) Confocal projections from control and *Fgfr2*cHet tracheae 5 weeks post-tmx. Green, GFP (*Rosa* reporter); red, KRT5 (basal cells); white, KRT8 (luminal cells); blue, DAPI (nuclei). Arrowheads indicate GFP$^+$ luminal cells. Arrows indicate GFP$^+$ basal cells. (B) Percentage of all GFP$^+$ cells 5 weeks post-tmx that are GFP$^+$, T1 α$^-$ (see Fig. 1D) or GFP$^+$, KRT8$^+$ (see A). (C) Sections from control and *Fgfr2*cHet tracheae 5 weeks post-tmx. Green, GFP (*Rosa* reporter); red, SCGB1A1 (club cells); white, MUC5AC (mucous). Arrows indicate club cells containing a low level of MUC5AC protein. (D) Percentage of all GFP$^+$ cells 5 weeks post-tmx that are GFP$^+$, SCGB1A1$^+$. (E) Confocal sections from control and *Fgfr2* cHet tracheae at 24 weeks post-tmx. Green, GFP (*Rosa* reporter); red, acetylated tubulin (cilia). Error bars indicate s.e.m. Scale bars: 20 µm in A,C; 25 µm in E.

Development (2017) 144, 1600-1606 doi:10.1242/dev.135681

(Fig. 3A). When analysed by genomic PCR, this resulted in an almost-pure population of *Fgfr2*$^{\Delta/+}$ cells (Fig. S3A,B). Four days after Ad-Cre-mediated deletion, we observed an increased proportion of KRT8^{+} cells in the *Fgfr2*cHet cultures (Fig. 3A-C). This recapitulates the *in vivo* phenotype and supports the conclusion that *Fgfr2*cHet BCs have a self-renewal defect. Additional cultures were

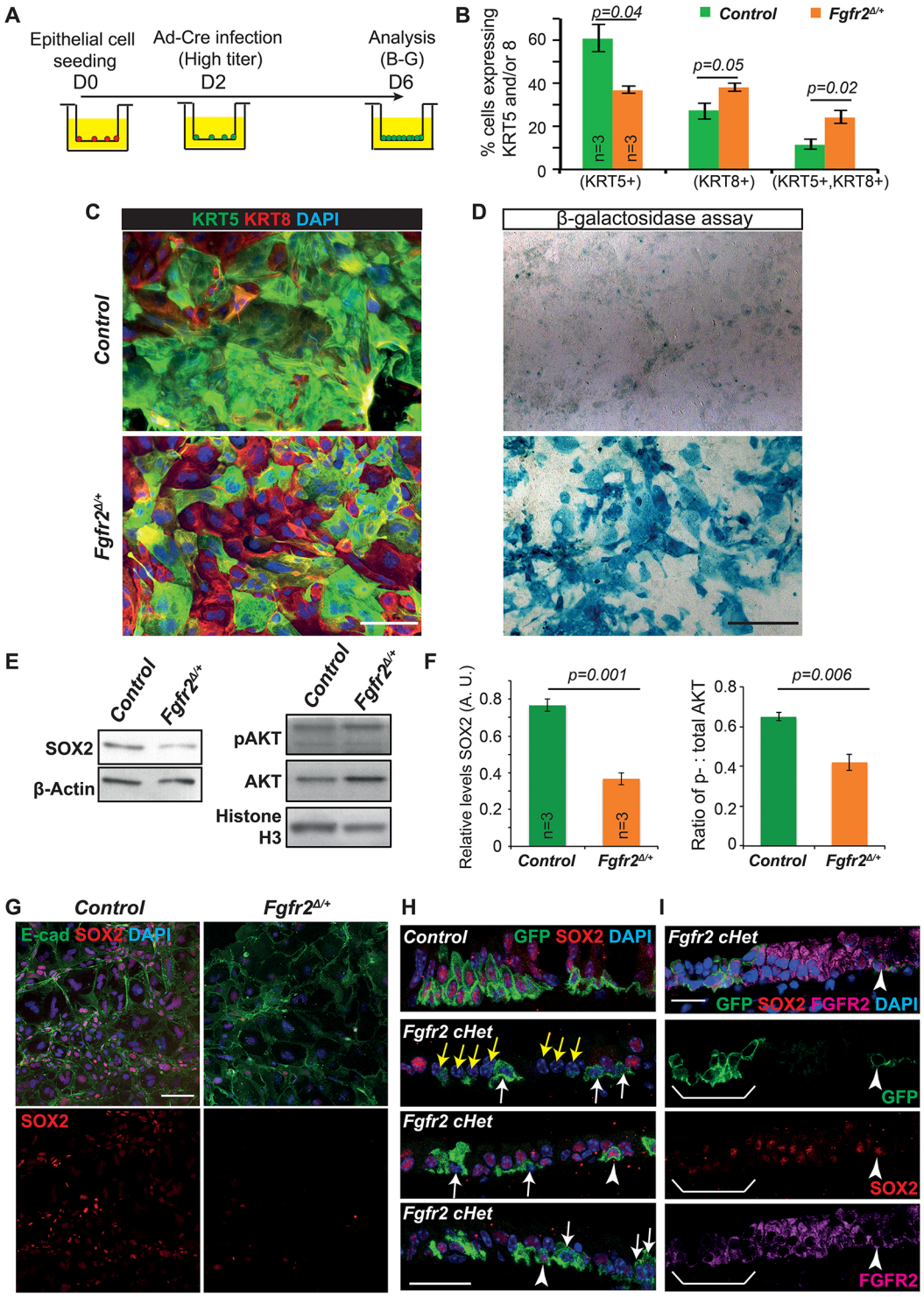

Fig. 3. *Fgfr2* conditional heterozygous basal cells have high levels of β-galactosidase and low levels of SOX2. (A) Experimental schematic for B-G. (B) Percentage tracheal epithelial cells at day 6 post-seeding expressing KRT5 and/or KRT8. (C,D) Control and *Fgfr2*cHet tracheal cells day 6 post-seeding. (C) Green, KRT5 (basal cells); red, KRT8 (luminal cells). (D) X-gal assay for β-galactosidase activity (blue pigment). (E) Representative western blots from control and *Fgfr2*cHet BCs. (F) Quantification of protein levels in E. (G) SOX2 in cHet BCs day 6 post-seeding. Green, E-cadherin (lateral cell membranes); red, SOX2. (H,I) Confocal images of control and *Fgfr2*cHet tracheal sections 5 weeks post-tmx. Green, GFP (*Rosa* reporter); red, SOX2; magenta, FGFR2. White arrows indicate lineage-labelled cells with decreased levels of SOX2. Arrowheads indicate lineage-labelled cells with no change in SOX2. Yellow arrows indicate unlabelled cells with decreased SOX2. Brackets in I indicate a patch of GFP^{+} cells that have decreased FGFR2 and no SOX2. Blue, DAPI. Error bars indicate s.e.m. Scale bars: 100 µm in C; 250 µm in D; 50 µm in G; 25 µm in H,I.

Development (2017) 144, 1600-1606 doi:10.1242/dev.135681

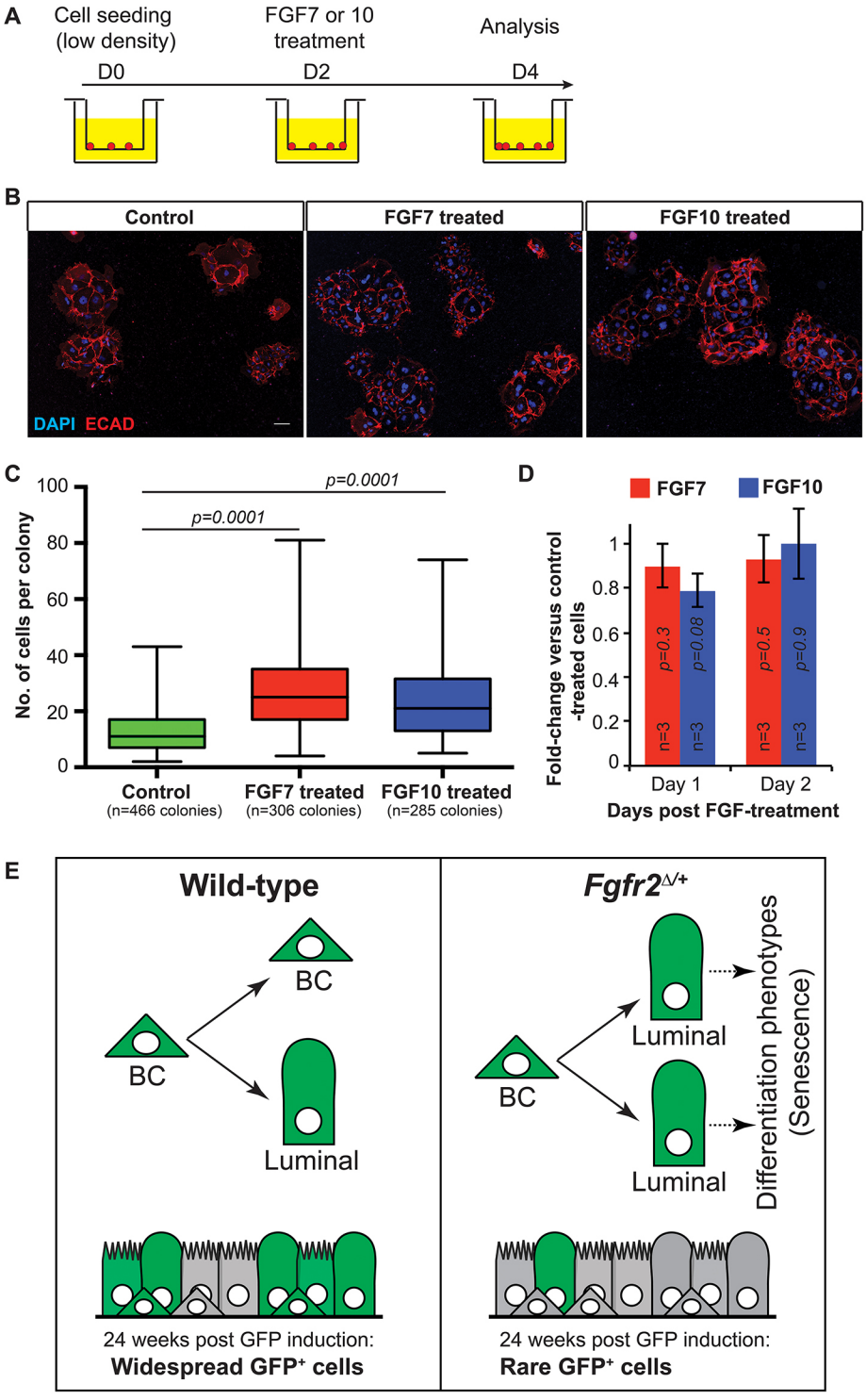

Fig. 4. FGF7 and FGF10 increase colony size of wild-type basal cells. (A) Experimental schematic. Epithelial cells plated at low density, 3×10^4 cells/insert. (B) Colonies formed by control, FGF7- or FGF10-treated wild-type cells. Red, E-cadherin; blue, DAPI. Scale bar: 100 µm. (C) Number of cells per colony in B. Data are mean±s.e.m. (D) Level of *Sox2* mRNA relative to control (normalized to 1) in cells treated with FGF7 or FGF10 for 1 or 2 days. Error bars indicate s.e.m. (E) *Fgfr2*cHet BCs rarely make self-renewing divisions in which a new BC is produced. Mutant BCs are more likely to produce descendants with luminal morphology/markers that are unable to completely differentiate, possibly because they senesce. The result is that GFP$^+$ *Fgfr2*cHet cells are gradually diluted out from both the basal and luminal populations, and the epithelium is sustained by GFP$^-$ wild-type BCs.

passaged and grown to confluence before differentiation at air-liquid interface (Fig. S4A-D). The *Fgfr2*cHet cells survived passaging but did not reach confluence and failed to express markers of ciliated or basal cell differentiation. Moreover, passaged cells were unable to grow in sphere-forming assays (Fig. S4E-H). The passaged *Fgfr2*cHet cells were somewhat enlarged and flattened, possibly indicating a senescent phenotype (Rodier and Campisi, 2011). We therefore tested for senescence-associated β-galactosidase activity in primary cultures of *Fgfr2*cHet cells. β-Galactosidase activity was detected in 3/3 *Fgfr2*cHet cultures and 0/3 controls (Fig. 3D). Senescence of the *Fgfr2*cHet cells *in vivo* could potentially explain why the luminal GFP$^+$ cells can express secretory markers, but do not later produce ciliated cells. However, we cannot absolutely exclude a luminal fate choice defect in *Fgfr2*cHet BCs.

Lower levels of SOX2 expression in the *Fgfr2* conditional heterozygous cells

We determined the effects of decreasing FGFR2 signalling on downstream pathways using immunoblotting. There was a 1.5-fold decrease in phosphorylated AKT in the *Fgfr2*$^{\Delta/+}$ cells (Fig. 3E,F),

Development (2017) 144, 1600-1606 doi:10.1242/dev.135681

but no change in phosphorylated ERK1/2 (Fig. S3C,D). These changes are consistent with a decrease in FGFR2 signalling via the PI3K-AKT pathway, which was implicated as the main pathway downstream of FGFR2 in adult small airway secretory cells and the developing trachea (Volckaert et al., 2011, 2013).

Most strikingly, there was a twofold decrease in SOX2 in the $Fgfr2^{\Delta/+}$ cells (Fig. 3E,F; Fig. S3C,D). We confirmed the decrease in SOX2 protein at a cellular level by *in vitro* immunostaining (Fig. 3G). Similarly, there was consistently lower SOX2 expression in GFP^+ cells in the *Fgfr2*cHet tracheae *in vivo* (Fig. 3H, arrows). As expected from the genetic strategy, in the mutants we also observed GFP^+, $SOX2^+$ cells (Fig. 3H, arrowheads) and GFP^-, $SOX2^-$ cells (Fig. 3H, yellow arrows), both are likely to have recombined only one floxed allele. Co-immunostaining with FGFR2 confirmed that the GFP^+, $SOX2^+$ cells observed in the mutants retained high levels of FGFR2 protein (Fig. 3I).

FGF7 and FGF10 can promote BC colony expansion *in vitro*

We predicted that if a decrease in *Fgfr2* results in loss of BC self-renewal, then activation of FGFR2 *in vitro* should promote the growth of BC colonies. FGF7 and FGF10 are expressed in homeostatic tracheae (Balasooriya et al., 2016) and are known to activate FGFR2 preferentially *in vitro* and *in vivo* (Ornitz et al., 1996). We plated wild-type BCs at low density and added FGF7 or FGF10 on culture day 2 after colonies were established (Fig. 4A). Addition of FGF7 or FGF10 had the opposite effect to decreasing *Fgfr2* and significantly increased colony size (Fig. 4B,C). Interestingly, FGF7 and FGF10 had no effect on the level of *Sox2* mRNA (Fig. 4D).

In conclusion, our data suggest that a normal function of FGFR2 signalling in adult airway BCs is to promote asymmetric self-renewing divisions (Fig. 4E). This is consistent with work in the embryonic trachea where ectopic FGF10 was observed to promote BC fate (Volckaert et al., 2013). By contrast, our previous work on FGFR1 in adult BCs showed that FGFR1 is required to inhibit steady-state proliferation and does not change the ability of BCs to self-renew (Balasooriya et al., 2016). Thus, FGFR1 and FGFR2 have independent functions in airway BCs. We cannot exclude the possibility that they also have other overlapping functions.

We also show that steady-state FGFR2 signalling is required, directly or indirectly, to maintain SOX2 protein levels in the adult airway. This is in contrast to the branching lung, where FGFR2 inhibits SOX2 expression at the tips. Interestingly, an FGFR2-SOX2 inductive relationship has been observed in other cell types (Mansukhani et al., 2005). An FGFR2-SOX2 relationship may be maintained in some squamous lung cancers where *FGFR2* and *SOX2* transcript levels are often correlated (Kim et al., 2016).

Haploinsufficiency of *Fgfr2* in conditionally deleted adult cells

We were surprised that our *Fgfr2*cHet BCs displayed striking phenotypes when germline $Fgfr2^{\Delta/+}$ animals are viable and fertile (Yu et al., 2003). We therefore looked for subtle epithelial defects in germline-deleted $Fgfr2^{\Delta/+}$ tracheae compared with wild-type siblings, but were unable to find any abnormalities (Fig. S5). *Fgfr2* is haploinsufficient in several organs, including the lacrimal and salivary glands (Shams et al., 2007). We suggest that in mouse embryos heterozygous for *Fgfr2*, genetic compensation operates in most tissues. However, conditional heterozygous deletion in the adult by-passes such mechanisms. This is very similar to recent findings from zebrafish genetics where genetic compensation has been found to operate in germline mutants, but not in acute knockdowns (Rossi et al., 2015). It raises the possibility that many genes that the mouse developmental community assume are uninteresting/redundant based on lack of germline knockout phenotypes do play important roles in development/homeostasis.

MATERIALS AND METHODS

Mice

Experiments were approved by local ethical review committees and conducted according to UK Home Office project licenses PPL80/2326 and 70/812. $Fgfr2^{fx}$ (Yu et al., 2003), *Tg(KRT5-CreER)* (Rock et al., 2009), *Rosa26R-fGFP* (Rawlins et al., 2009), $Gt(ROSA)26Sor^{tm1(CAG-tdTomato*,-EGFP*)Ees}$ (Prigge et al., 2013) and $Fgfr2^{\Delta/+}$ animals were generated by crossing $Fgfr2^{fx}$ to *Zp3-Cre* (de Vries et al., 2000). The genetic background was C57Bl/6J. Males and females >8 weeks old were used. The wild types were C57Bl/6J.

Tamoxifen

Adult (>8 week) animals were injected intraperitoneally four times, every other day, with 0.2 mg/g body weight tamoxifen.

Tracheal epithelial cell culture

Tracheal cells were isolated following published methods (Rock et al., 2009). Briefly, cells were incubated in Dispase II (Gibco, 16 U/ml) for 20 min at room temperature. Epithelial sheets were dissociated using 0.1% trypsin/EDTA. Unless otherwise stated, 5×10^4 cells in 0.5 ml MTEC/+ media (You et al., 2002) were plated on collagen-coated 12-well tissue culture inserts (BD Falcon, 353180). For tracheospheres, cells were passaged into 50% matrigel (Becton Dickinson). Adeno-Cre (University of Iowa, Gene Transfer Vector Core) was incubated at MOI 2500; vector pfu 1×10^6 for 8 h. Recombinant mouse FGF7 and FGF10 (R&D Systems) were used at 100 ng/ml. For competition assays, mixed populations of cells were grown to confluence and then imaged every 4 h for 10 days in a Nikon Biostation. Alternatively, confluent cultures were scratched and imaged every 2 h for 5 days. *In vitro* experiments were preformed in triplicate.

Immunostaining

Tracheae were fixed in 4% paraformaldehyde at 4°C for 4 h; washed PBS, sucrose protected, embedded in OCT (Optimum Cutting Temperature Compound, Tissue Tek) and sectioned at 6 µm. Airway culture inserts were washed in PBS, fixed for 10 min in 4% paraformaldehyde at room temperature and permeabilized with 0.3% Triton X-100. Primary antibodies are listed in Table S1. Alexa Fluor-conjugated secondary antibodies (1:2000) were from Life Technologies (Table S1). DAPI and fluoromount were from Sigma. X-gal staining was performed using Senescence β-galactosidase staining kit (Cell Signaling, 9860).

Microscopy and image scoring

Slides were imaged on a Zeiss AxioImager compound, or a Leica Sp8/Sp5 confocal microscope. Cells were scored manually in Fiji. For cryosections, every epithelial cell along the entire proximal to distal length of a longitudinal section from the centre of the trachea was scored. For cultured cells at least three random fields of view from each insert were scored. Raw cell counts are available in Fig. S6.

RT-qPCR

Primary tracheal epithelial cells were isolated and sorted using a fluorescence-activated cell sorting MoFlo flow cytometer. GFP^+ basal cells from control and *Fgfr2*cHet tracheae were sorted as GFP^+, GSIβ4 $lectin^+$ (Balasooriya et al., 2016). Total RNA was extracted using Qiagen RNEasy Mini Kit. Taqman gene expression assays for *Ppia* (Mm02342429_g1), *Fgfr2* (Mm01269930_m1) and *Sox2* (Mm03053810_s1) (Life Technologies) were used.

Immunoblots

Cells were collected in Cell Extraction Buffer (Invitrogen, FNN0011) with protease inhibitor (Roche 04693116001) and PMSF (Sigma, P7626). Proteins were separated on 10% or 12% SDS-PAGE gels before being transfer onto Millipore Immobilon-P PVDF Membrane (Merck Millipore, IPVH00010). Primary antibodies are listed in Table S1. Detection with

HRP-conjugated secondaries (Abcam, 1:10,000) and enhanced chemiluminescense (Thermo Scientific, PI-32109) was carried out. Quantitation is based on protein from three biological replicates separated on the same polyacrylamide gel. Band intensity was analysed in Fiji normalised to the loading control.

Statistics

P-values were obtained using an unpaired two-tailed student's *t*-test with unequal variance.

Acknowledgements

We thank Quitz Jeng and Jane Brady for technical assistance.

Competing interests

The authors declare no competing or financial interests.

Author contributions

G.I.B. designed and performed experiments, analysed data and edited the manuscript. M.G. designed, performed and analysed experiments. E.P. designed experiments and edited the manuscript. E.L.R. conceived and led the project, designed and performed experiments, analysed data, and wrote and edited the manuscript.

Funding

This study was supported by the Medical Research Council (G0900424 to E.R.). Core funders were as follows: Wellcome Trust (092096) and Cancer Research UK (C6946/A14492) supporting the Gurdon Institute; Wellcome Trust and Medical Research Council supporting the Stem Cell Initiative. Deposited in PMC for immediate release.

Supplementary information

Supplementary information available online at
http://dev.biologists.org/lookup/doi/10.1242/dev.135681.supplemental

References

Abler, L. L., Mansour, S. L. and Sun, X. (2009). Conditional gene inactivation reveals roles for Fgf10 and Fgfr2 in establishing a normal pattern of epithelial branching in the mouse lung. *Dev. Dyn.* **238**, 1999-2013.

Balasooriya, G. I., Johnson, J.-A., Basson, M. A. and Rawlins, E. L. (2016). An FGFR1-SPRY2 signaling axis limits basal cell proliferation in the steady-state airway epithelium. *Dev. Cell* **37**, 85-97.

Correia, L. L., Johnson, J. A., McErlean, P., Bauer, J., Farah, H., Rassl, D. M., Rintoul, R. C., Sethi, T., Lavender, P., Rawlins, E. L. et al. (2017). SOX2 drives bronchial dysplasia in a novel organotypic model of early human squamous lung cancer. *Am. J. Respir. Crit. Care. Med.* doi:10.1164/rccm.201510-2084OC.

de Vries, W. N., Binns, L. T., Fancher, K. S., Dean, J., Moore, R., Kemler, R. and Knowles, B. B. (2000). Expression of Cre recombinase in mouse oocytes: a means to study maternal effect genes. *Genesis* **26**, 110-112.

Ferone, G., Song, J.-Y., Sutherland, K. D., Bhaskaran, R., Monkhorst, K., Lambooij, J.-P., Proost, N., Gargiulo, G. and Berns, A. (2016). SOX2 is the determining oncogenic switch in promoting lung squamous cell carcinoma from different cells of origin. *Cancer Cell* **30**, 519-532.

Gontan, C., de Munck, A., Vermeij, M., Grosveld, F., Tibboel, D. and Rottier, R. (2008). Sox2 is important for two crucial processes in lung development: branching morphogenesis and epithelial cell differentiation. *Dev. Biol.* **317**, 296-309.

Hashimoto, S., Chen, H., Que, J., Brockway, B. L., Drake, J. A., Snyder, J. C., Randell, S. H. and Stripp, B. R. (2012). beta-Catenin-SOX2 signaling regulates the fate of developing airway epithelium. *J. Cell Sci.* **125**, 932-942.

Kim, B. R., Van de Laar, E., Cabanero, M., Tarumi, S., Hasenoeder, S., Wang, D., Virtanen, C., Suzuki, T., Bandarchi, B., Sakashita, S. et al. (2016). SOX2 and PI3K cooperate to induce and stabilize a squamous-committed stem cell injury state during lung squamous cell carcinoma pathogenesis. *PLoS Biol.* **14**, e1002581.

Mansukhani, A., Ambrosetti, D., Holmes, G., Cornivelli, L. and Basilico, C. (2005). Sox2 induction by FGF and FGFR2 activating mutations inhibits Wnt signaling and osteoblast differentiation. *J. Cell Biol.* **168**, 1065-1076.

Mori, M., Mahoney, J. E., Stupnikov, M. R., Paez-Cortez, J. R., Szymaniak, A. D., Varelas, X., Herrick, D. B., Schwob, J., Zhang, H. and Cardoso, W. V. (2015). Notch3-Jagged signaling controls the pool of undifferentiated airway progenitors. *Development* **142**, 258-267.

Ochieng, J. K., Schilders, K., Kool, H., Boerema-De Munck, A., Buscop-Van Kempen, M., Gontan, C., Smits, R., Grosveld, F. G., Wijnen, R. M., Tibboel, D. et al. (2014). Sox2 regulates the emergence of lung basal cells by directly activating the transcription of Trp63. *Am. J. Respir. Cell Mol. Biol.* **51**, 311-322.

Ornitz, D. M., Xu, J., Colvin, J. S., McEwen, D. G., MacArthur, C. A., Coulier, F., Gao, G. and Goldfarb, M. (1996). Receptor specificity of the fibroblast growth factor family. *J. Biol. Chem.* **271**, 15292-15297.

Prigge, J. R., Wiley, J. A., Talago, E. A., Young, E. M., Johns, L. L., Kundert, J. A., Sonsteng, K. M., Halford, W. P., Capecchi, M. R. and Schmidt, E. E. (2013). Nuclear double-fluorescent reporter for in vivo and ex vivo analyses of biological transitions in mouse nuclei. *Mamm. Genome* **24**, 389-399.

Que, J., Okubo, T., Goldenring, J. R., Nam, K.-T., Kurotani, R., Morrisey, E. E., Taranova, O., Pevny, L. H. and Hogan, B. L. M. (2007). Multiple dose-dependent roles for Sox2 in the patterning and differentiation of anterior foregut endoderm. *Development* **134**, 2521-2531.

Que, J., Luo, X., Schwartz, R. J. and Hogan, B. L. M. (2009). Multiple roles for Sox2 in the developing and adult mouse trachea. *Development* **136**, 1899-1907.

Rawlins, E. L. and Hogan, B. L. M. (2008). Ciliated epithelial cell lifespan in the mouse trachea and lung. *Am. J. Physiol. Lung Cell. Mol. Physiol.* **295**, L231-L234.

Rawlins, E. L., Ostrowski, L. E., Randell, S. H. and Hogan, B. L. M. (2007). Lung development and repair: contribution of the ciliated lineage. *Proc. Natl. Acad. Sci. USA* **104**, 410-417.

Rawlins, E. L., Okubo, T., Xue, Y., Brass, D. M., Auten, R. L., Hasegawa, H., Wang, F. and Hogan, B. L. M. (2009). The role of Scgb1a1+ Clara cells in the long-term maintenance and repair of lung airway, but not alveolar, epithelium. *Cell Stem Cell* **4**, 525-534.

Rock, J. R., Onaitis, M. W., Rawlins, E. L., Lu, Y., Clark, C. P., Xue, Y., Randell, S. H. and Hogan, B. L. M. (2009). Basal cells as stem cells of the mouse trachea and human airway epithelium. *Proc. Natl. Acad. Sci. USA* **106**, 12771-12775.

Rock, J. R., Randell, S. H. and Hogan, B. L. M. (2010). Airway basal stem cells: a perspective on their roles in epithelial homeostasis and remodeling. *Dis. Model. Mech.* **3**, 545-556.

Rodier, F. and Campisi, J. (2011). Four faces of cellular senescence. *J. Cell Biol.* **192**, 547-556.

Rossi, A., Kontarakis, Z., Gerri, C., Nolte, H., Hölper, S., Krüger, M. and Stainier, D. Y. R. (2015). Genetic compensation induced by deleterious mutations but not gene knockdowns. *Nature* **524**, 230-233.

Shams, I., Rohmann, E., Eswarakumar, V. P., Lew, E. D., Yuzawa, S., Wollnik, B., Schlessinger, J. and Lax, I. (2007). Lacrimo-auriculo-dento-digital syndrome is caused by reduced activity of the fibroblast growth factor 10 (FGF10)-FGF receptor 2 signaling pathway. *Mol. Cell. Biol.* **27**, 6903-6912.

Teixeira, V. H., Nadarajan, P., Graham, T. A., Pipinikas, C. P., Brown, J. M., Falzon, M., Nye, E., Poulsom, R., Lawrence, D., Wright, N. A. et al. (2013). Stochastic homeostasis in human airway epithelium is achieved by neutral competition of basal cell progenitors. *Elife* **2**, e00966.

Tompkins, D. H., Besnard, V., Lange, A. W., Wert, S. E., Keiser, A. R., Smith, A. N., Lang, R. and Whitsett, J. A. (2009). Sox2 is required for maintenance and differentiation of bronchiolar Clara, ciliated, and goblet cells. *PLoS ONE* **4**, e8248.

Tompkins, D. H., Besnard, V., Lange, A. W., Keiser, A. R., Wert, S. E., Bruno, M. D. and Whitsett, J. A. (2011). Sox2 activates cell proliferation and differentiation in the respiratory epithelium. *Am. J. Respir. Cell Mol. Biol.* **45**, 101-110.

Vivarelli, S., Wagstaff, L. and Piddini, E. (2012). Cell wars: regulation of cell survival and proliferation by cell competition. *Essays Biochem.* **53**, 69-82.

Volckaert, T., Dill, E., Campbell, A., Tiozzo, C., Majka, S., Bellusci, S. and De Langhe, S. P. (2011). Parabronchial smooth muscle constitutes an airway epithelial stem cell niche in the mouse lung after injury. *J. Clin. Invest.* **121**, 4409-4419.

Volckaert, T., Campbell, A., Dill, E., Li, C., Minoo, P. and De Langhe, S. (2013). Localized Fgf10 expression is not required for lung branching morphogenesis but prevents differentiation of epithelial progenitors. *Development* **140**, 3731-3742.

Watson, J. K., Rulands, S., Wilkinson, A. C., Wuidart, A., Ousset, M., Van Keymeulen, A., Göttgens, B., Blanpain, C., Simons, B. D. and Rawlins, E. L. (2015). Clonal dynamics reveal two distinct populations of basal cells in slow-turnover airway epithelium. *Cell Rep.* **12**, 90-101.

You, Y., Richer, E. J., Huang, T. and Brody, S. L. (2002). Growth and differentiation of mouse tracheal epithelial cells: selection of a proliferative population. *Am. J. Physiol. Lung Cell. Mol. Physiol.* **283**, L1315-L1321.

Yu, K., Xu, J., Liu, Z., Sosic, D., Shao, J., Olson, E. N., Towler, D. A. and Ornitz, D. M. (2003). Conditional inactivation of FGF receptor 2 reveals an essential role for FGF signaling in the regulation of osteoblast function and bone growth. *Development* **130**, 3063-3074.

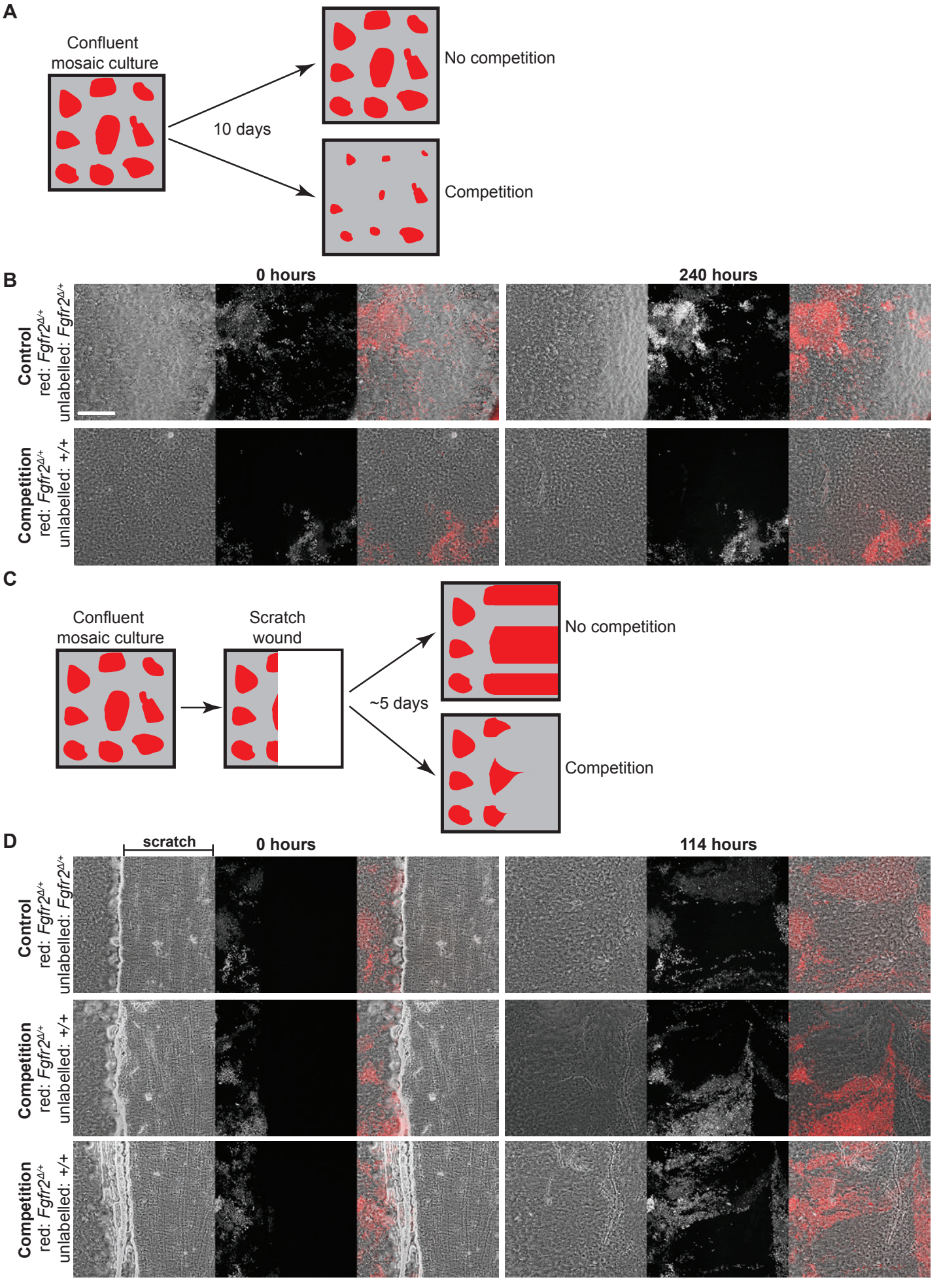

Figure S1. No evidence for cell competition between *Fgfr2*$^{\Delta/+}$ and *Fgfr2*$^{+/+}$ basal cells in vitro. (A) Experimental set-up in B. Freshly isolated basal cells were mixed at a 1:2 ratio, grown to confluence on cell culture inserts and imaged at intervals for 10 days. In cultures with no competition both cell populations will continue at the same ratio, whereas in cultures with competition the patch size of the "loser" cell population will decrease over time. (B) 0 and 240 hour frames from phase contrast/red channel time-lapse experiments. Upper panel: control experiment, red cells: *Fgfr2*$^{\Delta/+}$, unlabelled cells: *Fgfr2*$^{\Delta/+}$. Lower panel: competition experiment, red: *Fgfr2*$^{\Delta/+}$, unlabelled: *Fgfr2*$^{+/+}$. No evidence for competition was observed. (C) Experimental set-up in D. Freshly isolated basal cells were mixed at a 1:2 ratio, grown to confluence on cell culture inserts, mechanically wounded using a pipette tip and imaged at intervals for 5 days. In cultures with no competition labelled and unlabelled cells will contribute approximately equally to wound closure. In cultures with competition, the "loser" cell population will contribute less to wound closure. (D) 0 hour and 114 hour frames from phase contrast/red channel time-lapse experiments. Upper panel: control experiment, red cells: *Fgfr2*$^{\Delta/+}$, unlabelled cells: *Fgfr2*$^{\Delta/+}$. Lower panels: competition experiment, red cells: *Fgfr2*$^{\Delta/+}$, unlabelled cells: *Fgfr2*$^{+/+}$. No evidence for competition was observed. Bar = 0.5 mm in all panels. See also movies 1-5.

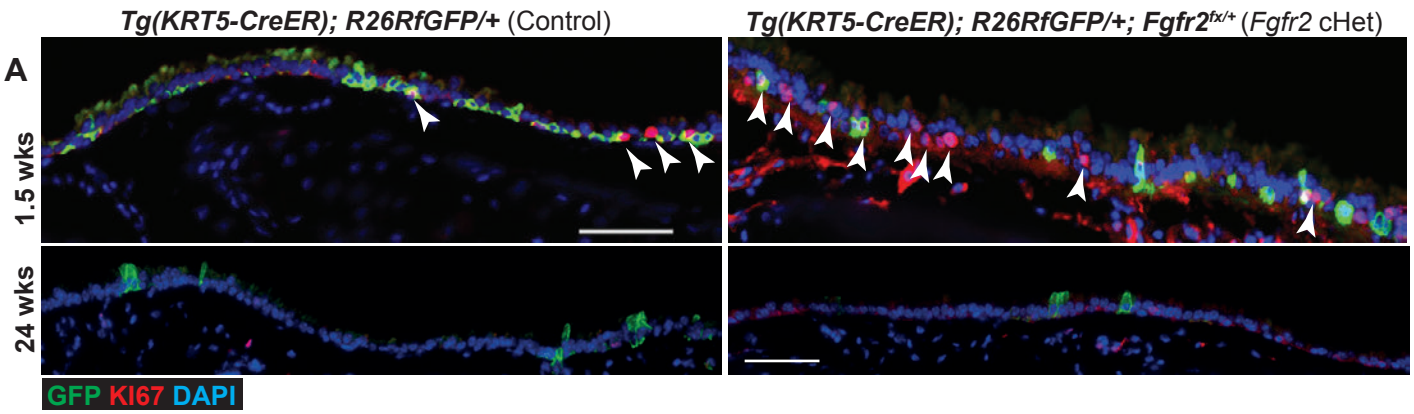

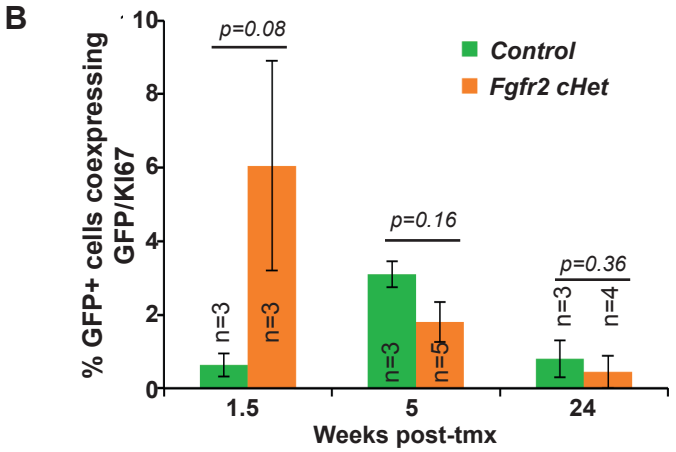

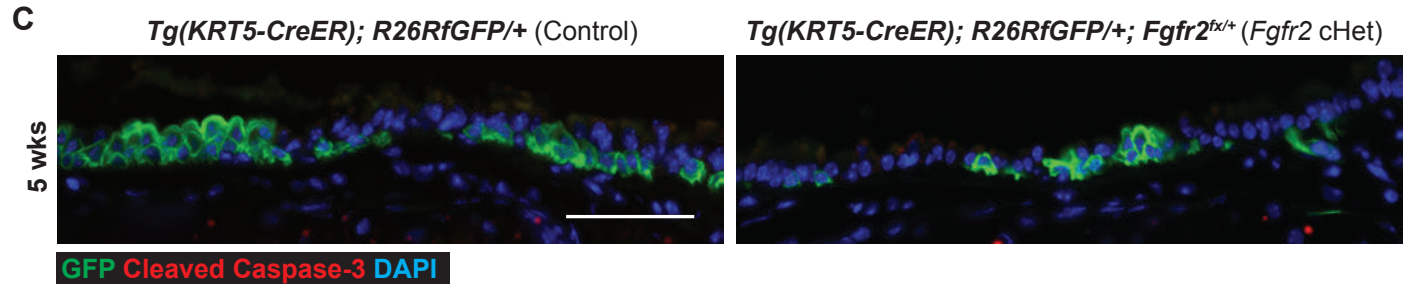

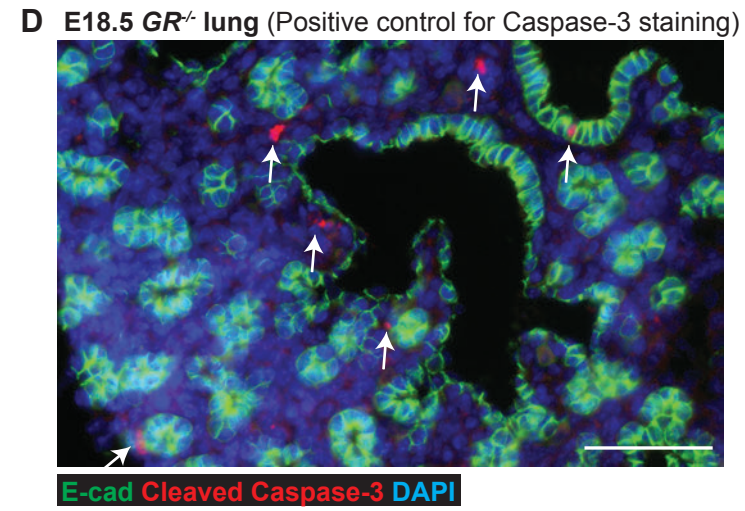

Figure S2. *Fgfr2* conditional heterozygous basal cells can proliferate and show no evidence of apoptosis. (A) Sections from control *Tg(KRT5-CreER); Rosa26R*$^{fGFP/+}$ and cHet *Tg(KRT5-CreER); Rosa26R*$^{fGFP/+}$*; Fgfr2*$^{fx/+}$ tracheae at 1.5 and 24 weeks post-tmx. Green: GFP (*Rosa* reporter); red: KI67 (proliferating cells); blue: DAPI (nuclei). Arrowheads mark KI67 positive cells. (B) Quantitation of the percentage of GFP^{+} cells that co-express KI67 throughout the experimental timecourse. Error bars = sem. (C) Sections from control *Tg(KRT5-CreER); Rosa26R*$^{fGFP/+}$ and cHet *Tg(KRT5-CreER); Rosa26R*$^{fGFP/+}$*; Fgfr2*$^{fx/+}$ tracheae at 5 weeks post-tmx. Green: GFP (*Rosa* reporter); red: Cleaved Caspase-3 (apoptotic cells); blue: DAPI (nuclei). (D) Section of E18.5 Glucocorticoid receptor null lung (GR$^{-/-}$, also known as *Nr3c1)* as a positive control for Cleaved Caspase-3 staining. Green: E-cadherin (lateral membranes); red: Cleaved Caspase-3 (apoptotic cells); blue: DAPI (nuclei). Scale bar = 50 μm in all panels.

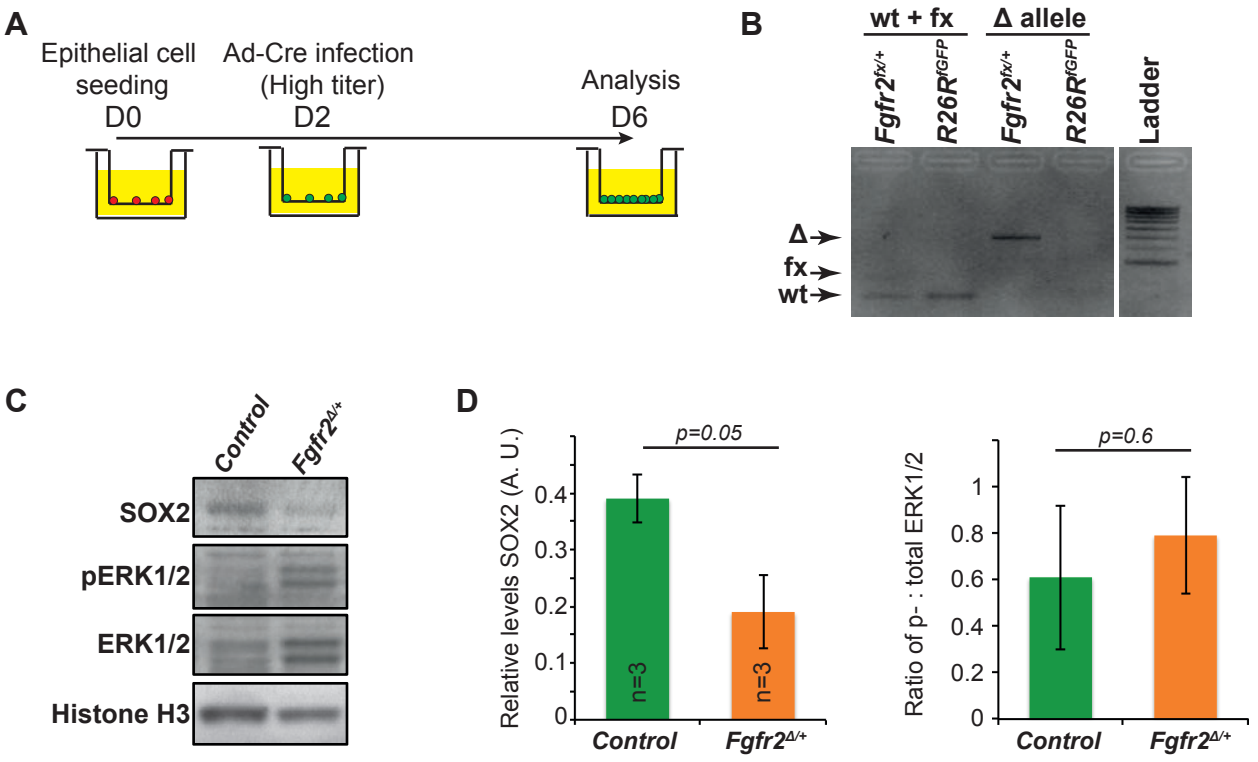

Figure S3. *Fgfr2* conditional heterozygous tracheal cells fail to terminally differentiate and self-renew in vitro

(A) Experimental schematic. Control (*Rosa26R*$^{fGFP/fGFP}$) and cHet (*Rosa26R*$^{fGFP/+}$*; Fgfr2*$^{fx/+}$) tracheal epithelial cells were seeded in BC expansion conditions and infected with Ad-Cre at day 2. On day 4 BCs were passaged onto new collagen-coated inserts for further expansion and ALI differentiation. (B) cHet BCs attach and proliferate post-passaging on collagen-coated inserts. (C, D) Control cultures form fully-differentiated monolayers containing multiciliated cells (C) and differentiated BCs (D) by 12 days post-seeding, but cHet BCs do not reach confluence and do not express differentiated markers in vitro. Arrows: fragmented nuclei, or multi-nucleate cells, seen in cHet cultures, but not controls. (E) Experimental schematic. Control (*Rosa26R*$^{fGFP/fGFP}$) and cHet (*Rosa26R*$^{fGFP/+}$*; Fgfr2*$^{fx/+}$) tracheal epithelial cells were seeded in BC expansion conditions and infected with Ad-Cre at day 2. On day 4 BCs were passaged into matrigel for sphere-forming assays. (F) Representative confocal sections of control and *Fgfr2 cHet* cultures 2 days post-seeding in matrigel. Green: KRT8; red: KRT5. (G) Images of control and *Fgfr2 cHet* tracheospheres 9 days post-seeding in matrigel. (H) Tracheosphere diameter, arbitrary units. Scale bars = 100 μm (B-D, G); 5 μm (F).

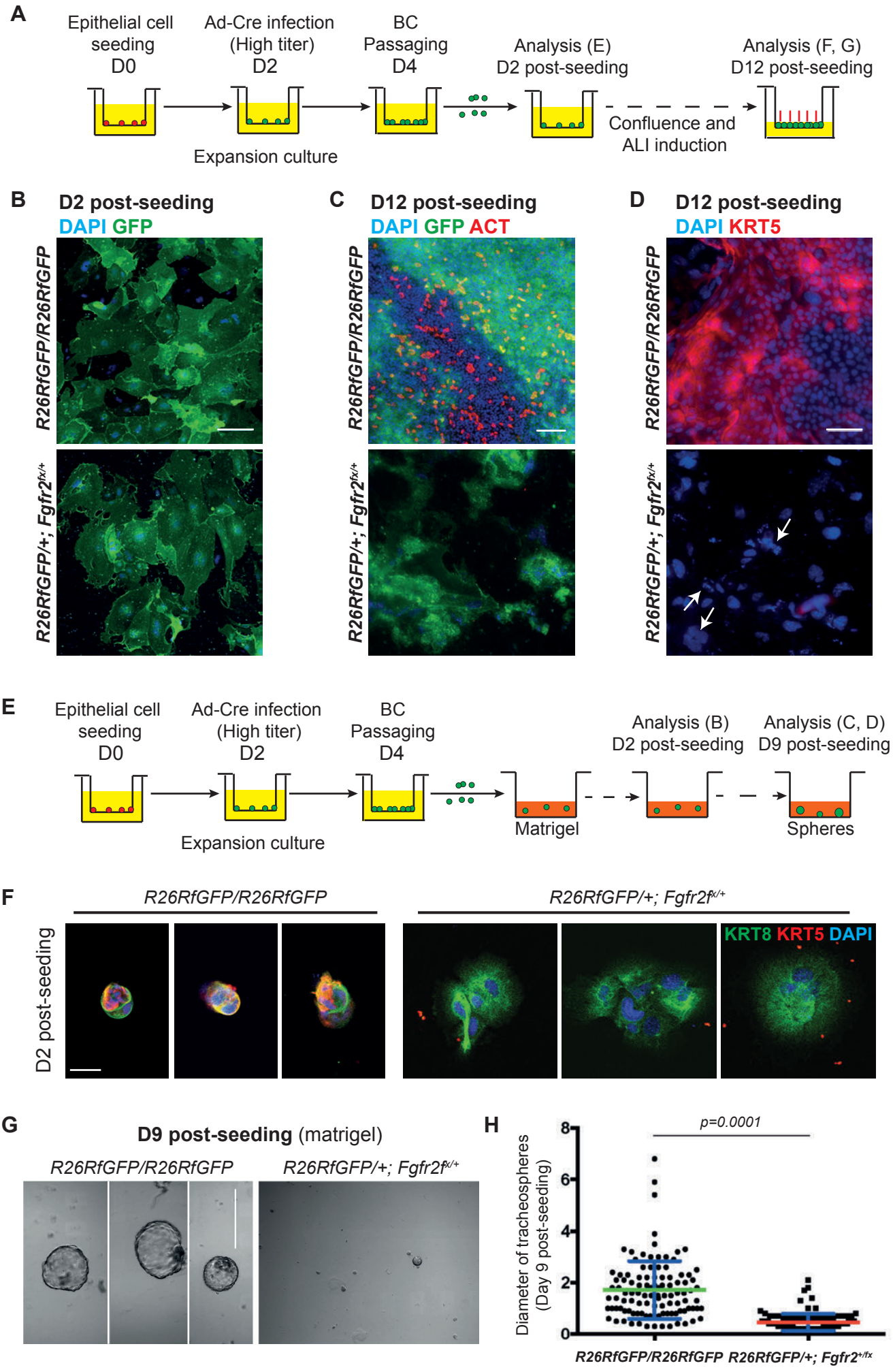

Figure S4. Decrease in FGFR2 signalling in vitro does not affect levels of MEK-ERK signalling. (A) Schematic of in vitro experimental time-course. (B) Representative genotyping (gDNA) PCR from *Rosa26R*$^{fGFP/fGFP}$ and *Rosa26R*$^{fGFP/+}$*; Fgfr2*$^{fx/+}$ viral-infected cells at day 6. Note that the cHet cells have efficient amplification of the wild-type (wt) and deleted (Δ) alleles, but very little amplification of the floxed (fx) allele indicating high levels of recombination in vitro. (C) Representative western blots from control and *Fgfr2* cHet day 6 basal cells showing levels of SOX2, pERK1/2, total ERK and Histone H3. (F) Quantification of protein levels in (E).

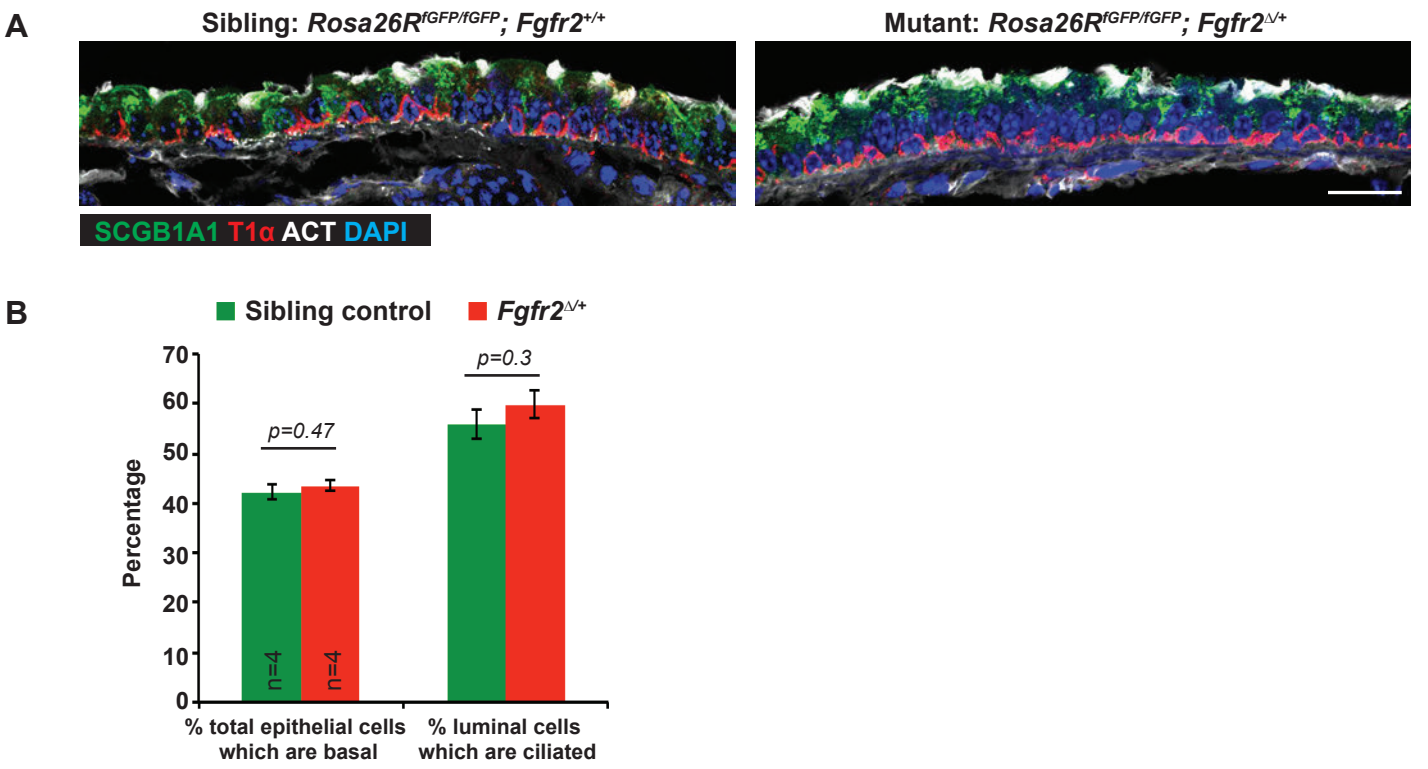

Figure S5. *Fgfr2*$^{\Delta/+}$ adult mice have a normal tracheal epithelium. (A) Representative sections from control *Rosa26R*$^{fGFP/fGFP}$ and sibling *Rosa26R*$^{fGFP/fGFP}$*; Fgfr2*$^{\Delta/+}$ tracheae. Green: SCGB1A1 (secretory cells); red: T1α (basal cells); white: acetylated tubulin (cilia); blue: DAPI. (B) Quantitation of the percentage of epithelial cells which are basal, and luminal cells which are ciliated in the two genotypes. Error bars = sem. Scale bar = 20 μm.

Fig. S6. Raw cell counts

***Fgfr2* conditional heterozygous cell counts**

Figure S2

		Total DAPI+ cells	Total GFP+ cells	KI67+,GFP- cells	KI67+,GFP+ cells	% of total GFP+ cells that are dual GFP+, KI-67+
1.5 weeks post-tmx						
1	*KRTS-CreER/+; R26-fGFP/+*	1033	64	6	0	0.0
2	*KRTS-CreER/+; R26-fGFP/+*	1469	96	24	1	1.0
3	*KRTS-CreER/+; R26-fGFP/+*	1024	228	6	2	0.9
4	*KRTS-CreER/+; R26-fGFP/+; Fgfr2 fx/+*	216	25	3	1	4.0
5	*KRTS-CreER/+; R26-fGFP/+; Fgfr2 fx/+*	1523	203	87	18	8.9
6	*KRTS-CreER/+; R26-fGFP/+; Fgfr2 fx/+*	1523	285	48	9	3.2
5 weeks post-tmx						
1	*KRTS-CreER/+; R26-fGFP/+*	1560	552	18	13	2.4
2	*KRTS-CreER/+; R26-fGFP/+*	1228	409	25	13	3.2
3	*KRTS-CreER/+; R26-fGFP/+*	1125	439	35	16	3.6
4	*KRTS-CreER/+; R26-fGFP/+*	/	/	/	/	/
5	*KRTS-CreER/+; R26-fGFP/+; Fgfr2 fx/+*	1171	408	22	11	2.7
6	*KRTS-CreER/+; R26-fGFP/+; Fgfr2 fx/+*	1071	218	9	2	0.9
7	*KRTS-CreER/+; R26-fGFP/+; Fgfr2 fx/+*	970	347	21	6	1.7
8	*KRTS-CreER/+; R26-fGFP/+; Fgfr2 fx/+*	1001	263	20	9	3.4
9	*KRTS-CreER/+; R26-fGFP/+; Fgfr2 fx/+*	1241	429	8	2	0.5
24 weeks post-tmx						
1	*KRTS-CreER/+; R26-fGFP/+*	1241	351	14	2	0.6
2	*KRTS-CreER/+; R26-fGFP/+*	1155	381	15	1	0.3
3	*KRTS-CreER/+; R26-fGFP/+*	1411	319	18	4	1.3
4	*KRTS-CreER/+; R26-fGFP/+; Fgfr2 fx/+*	1684	57	28	1	1.75
5	*KRTS-CreER/+; R26-fGFP/+; Fgfr2 fx/+*	1341	125	30	0	0.00
6	*KRTS-CreER/+; R26-fGFP/+; Fgfr2 fx/+*	1801	143	34	0	0.00
7	*KRTS-CreER/+; R26-fGFP/+; Fgfr2 fx/+*	1883	20	21	0	0.00

Figure 1

		Total DAPI+ cells	T1a+,GFP- cells	T1a+,GFP+ cells	T1a-,GFP+ cells	% of total T1a+ basal cells that are dual GFP+, T1a+	% of total luminal T1a- cells that are GFP+
		1164	564	80	1	14.18	0.17
		1907	934	201	5	21.52	0.51
		1573	789	307	7	38.91	0.89
		648	238	82	493	34.45	0.49
		1607	677	221	325	32.64	0.97
		1472	752	241	341	32.05	0.14
		1325	575	360	215	62.61	5.33
		1444	546	324	222	59.34	4.12
		1288	582	339	243	58.25	5.95
		/	/	/	/	/	/
		1283	583	234	349	40.14	5.57
		1149	441	151	290	34.24	6.07
		1505	733	276	457	37.65	14.51
		1451	529	212	317	40.08	4.45
		1195	685	301	384	43.94	19.22
		1659	592	216	130	36.49	12.18
		1155	608	188	420	30.92	29.43
		1517	799	152	647	19.02	21.87
		1766	587	7	580	1.19	3.39
		1081	472	32	440	6.78	8.21
		1787	710	31	679	4.37	11.23
		1940	829	9	820	1.09	1.35

Figure 2

GFP+, KS+ basal cells	GFP+, K8+ luminal	GFP+, KS-, K8- cells	GFP+, KS+, K8+ cells	% GFP+ columar cells from total GFP+
291	27	0	10	10
227	46	0	2	10.2
271	18	0	5	11
/	/	/	/	/
159	32	0	8	14.3
126	32	0	6	22.2
164	55	0	14	28.9
133	24	0	9	16.2
267	55	0	20	24.6

Figure 2

GFP+, SCGB1A1+ club cells	GFP+, MUCSAC+ goblet cells	GFP+, SCGB1a1-, MUCSAC- cells	GFP+, SCGB1A1+, MUCSAC+ cells	% GFP+ cells which are SCGB1A1+ club cells	GFP+, % GFP+ cells which are SCGB1A1+, MUCSAC- cells	GFP+, % GFP+ cells which are GFP+, SCGB1A1+, MUCSAC+
196	0	259	0	43.1	56.9	0
139	0	238	0	36.9	63.1	0
76	0	184	0	29.2	70.8	0
51	0	202	0	20.2	79.8	0
31	0	82	0	27.4	72.6	0
30	0	44	0	40.5	59.5	0
119	0	109	0	52.2	47.8	0
63	0	94	1	39.9	59.5	0.6
139	0	135	2	50.4	48.9	0.7

***Fgfr2* germline heterozygous cell counts**

Figure S5

	Total basal cells	Total ciliated cells	Other cells	Total luminal cells	% of total epithelial cells which are basal	% of total luminal cells which are ciliated
Rosa26R-fGFP; Fgfr2+/+	340	354	219	416	44.97	61.78
Rosa26R-fGFP; Fgfr2+/+	504	576	417	783	39.16	58.01
Rosa26R-fGFP; Fgfr2+/+	595	535	479	862	40.84	52.76
Rosa26R-fGFP; Fgfr2+/+	648	782	424	939	43.63	50.82
Rosa26R-fGFP; Fgfr2D/+	592	497	481	765	40.83	64.84
Rosa26R-fGFP; Fgfr2D/+	583	513	438	752	43.67	53.94
Rosa26R-fGFP; Fgfr2D/+	716	755	555	874	45.03	57.63
Rosa26R-fGFP; Fgfr2D/+	548	635	375	695	44.09	62.87

***Fgfr2* in vitro cell counts**

Figure 3

	KS+, K8- cells	KS-, K8+ cells	KS+, K8+ cells	KS-, K8- cells	% of total cells which are KS+, K8-	% of total cells which are KS-, K8+	% of total cells which are KS+, K8+
Rosa26R-fGFP/ Rosa26R-fGFP	1107	670	337	7	52.2	31.6	15.9
Rosa26R-fGFP/ Rosa26R-fGFP	814	797	424	10	60.4	28.8	10.5
Rosa26R-fGFP/ Rosa26R-fGFP	1001	297	124	0	70.4	20.9	8.7
Rosa26R-fGFP/+; Fgfr2fx/+	996	476	174	5	39.8	39	20.7
Rosa26R-fGFP/+; Fgfr2fx/+	813	930	521	18	35.6	40.8	22.8
Rosa26R-fGFP/+; Fgfr2fx/+	570	564	461	3	35.7	35.3	28.8

Movies

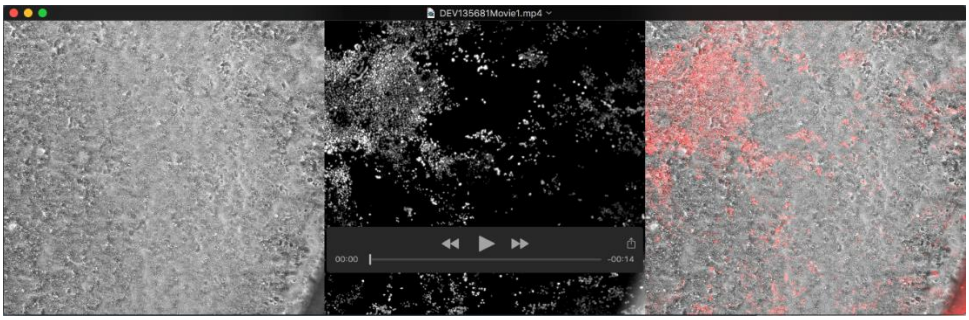

Movie 1. In vitro cell competition at confluence, control culture. Red cells: *Fgfr2*$^{\Delta/+}$, unlabelled cells: *Fgfr2* $^{\Delta/+}$. Confluent culture imaged every 4 hours for 10 days in a Nikon Biostation. Cell clones do not change in size; no evidence for cell competition.

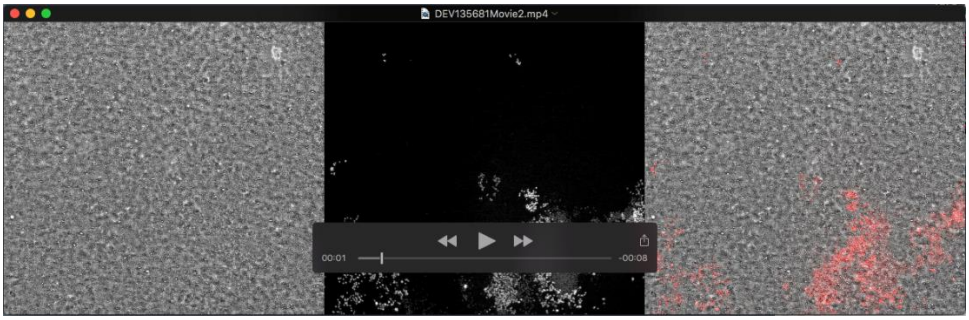

Movie 2. In vitro cell competition at confluence, experimental culture. Red cells: *Fgfr2*$^{\Delta/+}$, unlabelled cells: *Fgfr2* $^{+/+}$. Confluent culture imaged every 4 hours for 10 days in a Nikon Biostation. Cell clones do not change in size; no evidence for cell competition.

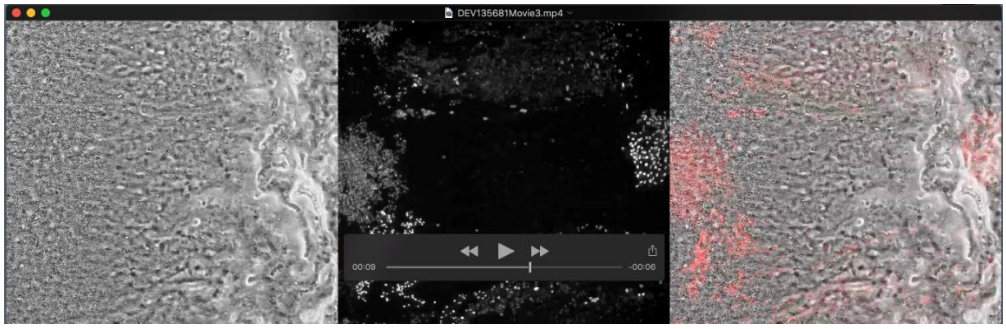

Movie 3. In vitro cell competition following wounding, control culture. Red cells: *Fgfr2*$^{\Delta/+}$, unlabelled cells: *Fgfr2*$^{\Delta/+}$. Confluent culture was wounded and then imaged every 2 hours for 5 days in a Nikon Biostation. Both cell populations expand into the wound equally; no evidence for cell competition.

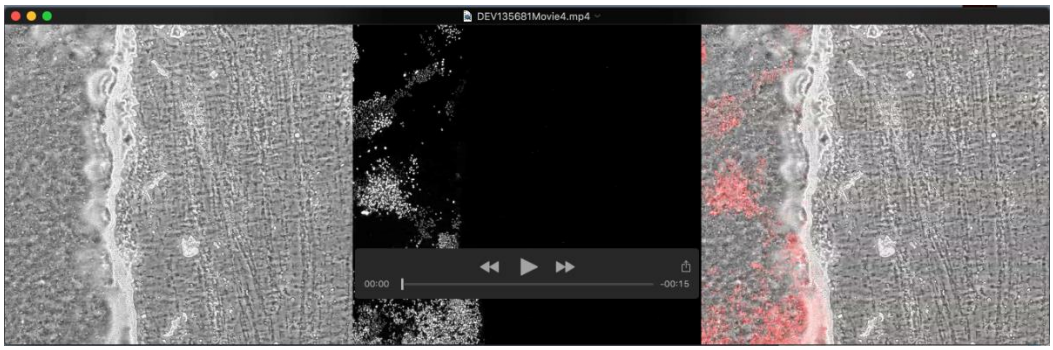

Movie 4. In vitro cell competition following wounding, experimental culture 1. Red cells: *Fgfr2*$^{\Delta/+}$, unlabelled cells: *Fgfr2*$^{+/+}$. Confluent culture was wounded and then imaged every 2 hours for 5 days in a Nikon Biostation. Both cell populations expand into the wound equally; no evidence for cell competition.

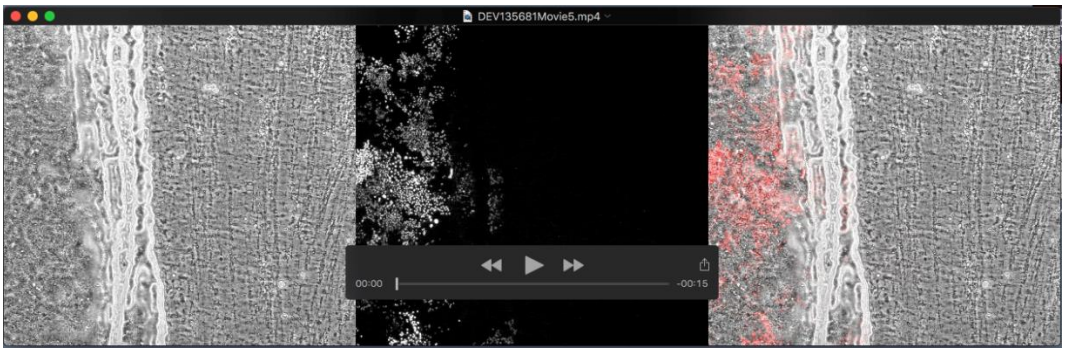

Movie 5. In vitro cell competition following wounding, experimental culture 2. Red cells: *Fgfr2*$^{\Delta/+}$, unlabelled cells: *Fgfr2* $^{+/+}$. Confluent culture was wounded and then imaged every 2 hours for 5 days in a Nikon Biostation. Both cell populations expand into the wound equally; no evidence for cell competition.

Table S1. Antibodies

Primary antibodies used for immunostaining on tissue sections or cells

Protein	Species	Dilution Factor	Antigen Retrieval*	Company	Order number/clone
Acetylated tubulin	Mouse	1:3000	No	Sigma	T7451
Cleaved Caspase-3	Rabbit	1:100	No	AbCam	ab2302
E-cadherin	Rat	1:3000	No	Thermofisher	13-1900
FGFR2	Rabbit	1:200	No	Santa Cruz	sc-122
GFP	Chick	1:1000	No	AbCam	AB13970
Keratin5	Rabbit	1:500	No	Covance	PRB-160P
Keratin8	Rat	1:200	No	DSHB	TROMA-1
KI67	Mouse	1:200	Yes	BD	550609
MUC5AC	Mouse	1:500	No	Thermofisher	MS-145P0
SCGB1A1	Goat	1:400	No	Santa Cruz	sc9772
SOX2	Goat	1:200	No	Santa Cruz	clone Y-17
T1α	Hamster	1:1000	No	DSHB	8.1.1

*Antigen retrieval by boiling tissue sections in 10 mM sodium citrate, pH 8 for Ki67.

Primary antibodies used for western blot

Protein	Dilution Factor	Company	Order number/clone
p-Akt(S473)	1:3000	Cell Signalling	3787
Akt (pan)	1:1000	Cell Signalling	4691
dpErk1/2	1:300	Cell Signalling	4370
Erk1/2 (total)	1:300	Cell Signalling	4695
SOX2	1:3000	AbCam	ab97959
Histone H3	1:10000	AbCam	ab39655
β-actin	1:50000	Sigma	A3854

Fluorescent secondary antibodies

All at 1:2000 from ThermoFisher Scientific (Molecular Probes)

Donkey anti-mouse 488	A21202
Goat anti-chick 488	A11039
Donkey anti-goat 488	A11055
Donkey anti-rabbit 488	A21206
Donkey anti-mouse 546	A10036
Donkey anti-rabbit 546	A10040
Donkey anti-goat 555	A21432
Goat anti-hamster 568	A21112
Donkey anti-rat 594	A21209
Donkey anti-mouse 647	A31571
Donkey anti-rabbit 647	A31573
Goat anti hamster 647	A21451
Goat anti-rat 647	A21247